

A Traveling Wave Fault Location Method for Earth Faults Based on Mode Propagation Time Delays of Multi-measuring Points

Abstract. A new traveling wave fault location method for earth faults is proposed based on propagation time delays between aerial mode and earth mode acquired by multi-measuring points on transmission line. Using phase-mode transformation theory and the theory of wavelet singularity detection to achieve the algorithm of propagation time difference detection. The JMarti model is used to build the system simulation model in the EMTP. The final results show that the method has high reliability and precision.

Streszczenie. Przedstawiona nową metodę wykrywania i lokalizacji błędu w linii transmisyjnej bazującą na analizie propagacji fali. Do tego celu wykorzystano transformację falkową. (Lokalizacja błędu w linii transmisyjnej na podstawie analizy propagacji fali)

Keywords: transmission line; traveling wave; mode propagation time delays; fault location

Słowa kluczowe: linia transmisyjna, fala wędrująca, lokalizacja błędu.

Introduction

Earth faults in power network have a very high probability of occurrence, up to 90%. The accurate and fast location of earth faults can not only reduce outage losses but also guarantee the safe and stable operation of the power system.

After earth faults occur to the transmission line, the transient traveling wave resulting from fault points includes not only aerial mode component but also earth mode component. Fault location is conducted through judgment of the approximate entropy of transient earth mode current of adjacent measuring points in literature [1]. However, this method is only capable of determining fault section, but can't determine the position of fault points. Another method is the single ended method which uses time delay of the initial wave head (hereinafter referred to as mode propagation time delays), the earth-mode and aerial-mode wave velocity to range. Although the method was put forward earlier, its location range is very limited due to the attenuation of earth mode and other problems.

The relationship between fault distance and mode propagation time delays is determined based on the change rules of earth mode wave velocity with fault distance, and a new travelling wave fault location scheme using the mode propagation time delays of multi-measuring points is realized. Fault current travelling wave is detected directly by detection device using Rogowski coil so that the traditional electromagnetic CT coil saturation, high frequency characteristics difference and the precision of head wave detection can be effectively improved. Because only the initial head wave of aerial mode and earth mode of each measuring point require judgment, the influence of line branch points can be almost eliminated.

Basic principle

As shown in Fig.1, an earth fault occurs at F point on line MN, the aerial mode and earth mode travelling wave generated from the fault point spread to the measuring point i by velocity v_1 and v_0 ($v_1 > v_0$) respectively.

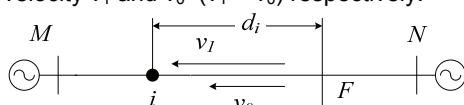


Fig. 1 Schematic diagram of zero-mode and aerial-mode traveling wave propagation in the case of earth fault

According to the theoretical analysis, the relationship between the physical length d'_i of the line from the fault

point to the measuring point i and the propagation time delay Δt_i for the modes' arrival at the measuring point is as follows:

$$(1) \quad d'_i = \frac{v_1 v_0}{v_1 - v_0} \Delta t_i$$

When the transmission line tower span is close to the sag, the physical length of the line can be regarded as that achieved [3] through the magnification of the field line length by a certain coefficient ϵ ($\epsilon > 1$), thus

$$(2) \quad d'_i = \epsilon d_i$$

Where d_i is the field line length from fault point F to the measuring point i . By substituting Formula (2) into Formula (1),

$$(3) \quad d_i = \frac{v_1 v_0}{\epsilon(v_1 - v_0)} \Delta t_i$$

It is easy to find from Formula 3 that there exists certain relation between the fault distance from the fault point to the measuring point (referring to the field line length) and the mode propagation time delay of this measuring point. This relation is subject to the influence of ϵ, v_1, v_0 and other factors. As far as a given line is concerned, ϵ can be regarded as a constant coefficient, and the line mode wave velocity v_1 is stable or can be regarded as constant, but earth mode wave velocity v_0 changes greatly [4]. Therefore, the relationship between fault distance and mode transmission time delay should be determined to estimate fault point position from mode transmission time delay. The earth mode wave velocity needs to be analyzed first.

Fault distance estimation method based on the mode transmission time delay.

Analysis of the variation of the earth mode wave velocity

The propagation process of earth mode component involves zero sequence parameters of the transmission line, because the earth mode resistance and inductance change greatly with the frequency, so it results in the great change of the earth mode wave velocity with the frequency.

Studies show [5] that, the earth mode wave velocity increases in a monotonous manner with frequency variation. Each frequency component of the earth mode traveling wave reaches the measuring point according to a decreasing order. The fast attenuation of high frequency component in the process of propagation results in the fact

that the longer the fault distance, the lower the highest frequency of the earth mode wave head and the smaller its corresponding wave velocity is.

To sum up, the earth mode wave velocity decreases with the increase of fault distance, and for a given line, the earth mode wave velocity is only related to fault distance, and not subjected to the influence of other factors [6]. The relationship between the two can be expressed as

$$(4) \quad v_0 = f(d)$$

where: f is the function of the earth mode wave velocity of fault distance d , which is a monotonically decreasing function. Fig.2 shows the relationship between earth mode wave velocity and fault distance.

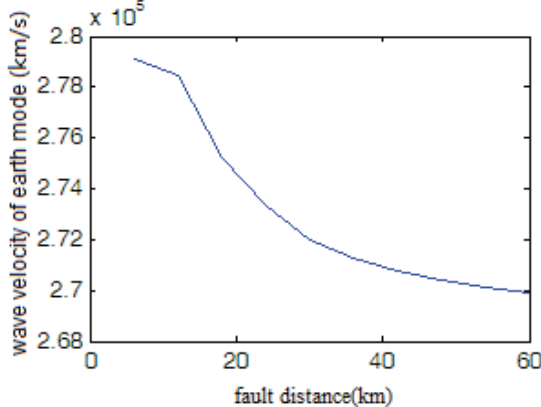


Fig. 2 The relation between earth mode wave velocity and fault distance

Fault distance estimation methods.

It can be easily known from Formula 3 and 4 that the fault distance d can be expressed as follows:

$$(5) \quad d = \frac{v_1 f(d)}{\epsilon(v_1 - f(d))} \Delta t$$

Where: Δt refers to the mode propagation time delay, while both ϵ and v_1 can be considered as constant.

It is not difficult to deduce the relation between Δt and d based on Formula (5):

$$(6) \quad \Delta t = \epsilon d \left(\frac{1}{f(d)} - \frac{1}{v_1} \right)$$

It can be known through the analysis of Formula (6) that, when fault distance d increases, then $f(d)$ decreases and $\frac{1}{f(d)} - \frac{1}{v_1}$ increases, thus Δt also increases. That is to say, the relationship between the mode transmission time delay Δt and the fault distance d can be expressed as follows:

$$(7) \quad \begin{cases} \Delta t = g(d) \\ d = g^{-1}(\Delta t) \end{cases}$$

where, both g and g^{-1} are monotonic decreasing function.

Based on the above analysis, it is not hard to find that, the farther the fault distance from the fault point to the measuring point is, the longer the mode propagation time delay tested at the measuring point is, and vice versa. So, the mode propagation time delay has one-to-one correspondence with the fault distance, that is, the known mode propagation time delay of the measuring point can be used to discover the corresponding fault distance based on the function g^{-1} .

As it is difficult to determine the function g^{-1} directly, the fitting method can be adopted to obtain relevant value. Fig.3

shows the curve about the relationship between fault distance and the mode transmission time delay. For a given line, corresponding $d-\Delta t$ curve can be obtained through EMTP simulation by setting relevant line structure parameters. The mode transmission time delay obtained at the measuring point, together with the $d-\Delta t$ graph, can be used to find out the fault distance from fault point to the measuring point.

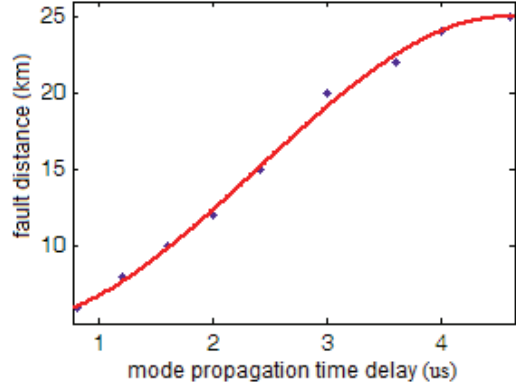


Fig. 3 Curve of fault distance and mode transmission time delay

Wave head detection of earth mode and aerial mode

It can be known based on the previous analysis that the mode propagation time delay Δt , which can be used to estimate fault distance, is key to fault location. In other words, the effective differentiation between wave head of earth mode and aerial mode at the measuring point the location of the time differences of the two directly influences the location results.

Sampling and storage of fault current travelling wave

The traveling wave detection device installed at each measuring point mentioned in this paper uses Rogowski coil to extract fault current travelling wave. The isolated measurement of high voltage circuit can be easily achieved as there is no direct connection [7] between Rogowski coil and the line measured.

The traveling-wave signal of high frequency collected by Rogowski coil reaches high-speed A/D converter via the signal conditioning circuit, which is controlled by CPLD. Once the line breaks down, CPLD starts high-frequency sampling immediately, and writes sampled data successively into SRAM.

After the completion of sampling and storage, CPLD promptly notifies CPU to read sampled data and carry out phase-mode transformation, wavelet transform and related data processing, so as to test the wave head of aerial mode and earth mode.

Phase-mode transformation

The complex electromagnetic coupling relationship exists in the three-phase transmission lines. For the purpose of simplifying calculation, phase-mode transformation is usually used for decoupling. The commonly-used transformation matrices include Clarke, Karenbauer, and many others, but these matrices all have certain defects. Mode 1 or 2 alone is not enough to represent all fault types. In literature [8] a new phase-mode transformation matrix Q^{-1} is proposed. This matrix enables the existence of a single aerial mode in all types of fault. The transform formula is as follows:

$$(8) \quad i_m = Q^{-1} i$$

$$Q^{-1} = \begin{bmatrix} 1 & 1 & 1 \\ 1 & 2 & -3 \\ 1 & -3 & 2 \end{bmatrix}$$

(9)

Where: $i_m = [i_{(0)}, i_{(1)}, i_{(2)}]^T$ is the mode; $i_{(1)}, i_{(2)}$ is mode 1 and 2, respectively, collectively called aerial mode; $i_{(0)}$ is the earth mode; $i = [i_A, i_B, i_C]^T$ is the three-phase phasor A, B and C.

After the aerial mode and earth mode components are obtained through phase-mode transformation, the high-frequency signals can be extracted from different mode components to test the respective wave head.

Dyadic wavelet transform

Dyadic wavelet has the time-shift covariance of the continuous wavelet transform, but the computation is greatly reduced because the scale measurement is discretized and the normal frequency shaft is divided into adjacent frequency bands. As a consequence, it is especially suitable for the analysis of the non-stationary signal as traveling wave [9]. The wavelet transform result of each scale is the component of the signal in the corresponding frequency band. The higher the scale, the lower the frequency is.

Dyadic frequency band of the signal can be divided using a pair of mirror filter $\{\bar{h}_n\}$ and $\{\bar{g}\}$, which can also achieve the multi-scale decomposition. The algorithm is briefly introduced below. If $c_0(n)$ is the original signal, the discrete approximate signal $c_1(n)$ and discrete detail signal $d_1(n)$ at scale 1 can be obtained using the Formula (10) and (11).

$$(10) \quad c_1(n) = \sum_k \bar{h}(2n-k)c_0(k)$$

$$(11) \quad d_1(n) = \sum_k \bar{g}(2n-k)c_0(k)$$

$c_2(n)$ and $d_2(n)$ at scale 2 can be obtained by replacing $c_0(n)$ with $c_1(n)$. The rest may be deduced by analogy [10].

The performance of the signal on different frequency bands can be observed after wavelet transform over the signal to realize feature extraction.

Singularity detection

The modulus maxima of wavelet transform usually corresponds to the single singularity and can be used in singularity detection. The concrete definition is given as follows:

$W_s f(x)$ is the wavelet transform of the function $f(x)$. If at the scale S , $|W_s f(x)| \leq |W_s f(x_0)|$ can be deduced for all $x \in (x - \delta, x + \delta)$ at a particular domain of x_0 , x_0 is the modulus maximum point of wavelet transform and $W_s f(x_0)$, the modulus maxima [11].

It should be noted that noise signal and traveling wave signal is very similar, and also has singularity. Thus, noise elimination should be considered in wave head detection. Multi-scale singularity detection of the signal can be realized through wavelet transform, and traveling wave signal de-noising can be realized taking advantage of different performance characteristics of traveling wave and noise on different scales [12]. In Fig.4, the noise signal at the scale 1 completely submerges travelling wave signal, but its maximum value at scale 2 is less than one-fourth of the initial wave head amplitude of traveling wave, while the noise at scale 3 is very weak. With the increase of the scale, the wavelet transform results of the noise quickly attenuate, and the modulus maxima of wavelet transform of

the traveling wave signal increases. According to this characteristic, the wave head of travelling wave at relatively high scale can be roughly located, and then the precision location within the range of the rough location using the detection result at low scale can be achieved[13].

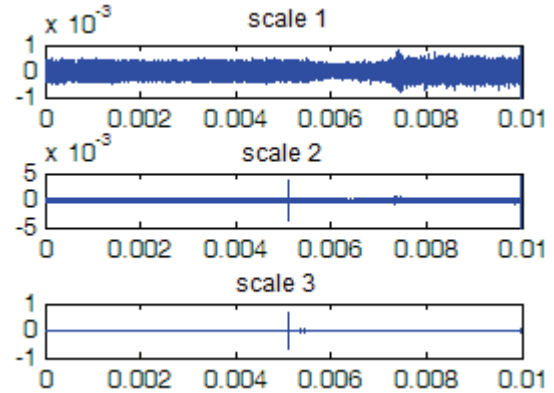


Fig. 4 Wavelet transform in signal denoising

The wavelet transform is performed over aerial mode and earth mode, respectively, and the time corresponding to their first respective modulus maxima are the arrival time for the initial wave head of aerial mode and earth mode. From this, the mode transmission time delays of the two can be obtained.

Realization of the comprehensive fault location using multiple measuring points System constitution

The fault location system in this paper is composed of several measuring points on the transmission line and one monitoring station, as shown in Fig.5. There are n ($n \geq 2$) measuring points on line MN, and at each measuring point a traveling wave detection device is installed to detect initial wave head of aerial mode and earth mode.

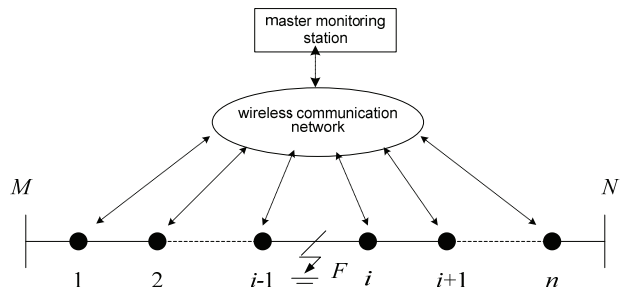


Fig. 5 System structure

The arrangement of the measuring points on the line can be selected according to the actual situation. Considering the large attenuation of earth mode component (based on EMTP simulation results, it is difficult to detect wave head of earth mode 30 km away from the fault point at scale 2, or 60 km away at scale 4). The field line length between adjacent measuring points should not be too long.

The measuring point (referred to as effective node hereinafter) capable of detecting the wave head of earth mode can upload time delay information by means of GSM/GPRS to the monitoring station, where all the information uploaded is comprehensively analyzed and processed to determine the fault point position.

Preliminary location of fault points

According to the principle that the shorter the fault distance, the smaller the mode propagation time delay is, the master station ranks the time delay of s effective nodes

collected. If the time delay $\Delta t_{\text{uploaded}}$ by the measuring point i is the smallest, it can be judged that the fault point is near the measuring point i .

Precise location of fault points

The range of fault point can be determined preliminarily after the measuring point i nearest to the fault point is found. Meanwhile, the fault direction of the remaining $s-1$ effective nodes can also be made clear, that is, whether any point other than i is located in the upstream (near to the first end M) or the downstream of the fault point. Suppose that t_j is the mode propagation time delay uploaded by $j \neq \text{node}$, and the fault distance d_j corresponding to t_j can be estimated according to the curve in Fig.3. d_j can be converted into d_j^* , the fault distance from the fault point to the end M:

$$(12) \quad d_j^* = L_j + d_j$$

$$(13) \quad d_j^* = L_j - d_j$$

Formula (12) and (13) correspond to the situation when node j is located at the upper stream and down stream of the fault point, respectively. In the formulas, L_j refers to the field line length from the measuring point j to the end M.

The fault distance d_F can be calculated by taking the mean value of the sum of all d_j^*

$$(14) \quad d_F = \frac{\sum_{j=1}^{s-1} d_j^*}{s-1}$$

EMTP simulation study

In this paper, simulation modeling is conducted over 110kV dual-terminal power system using EMTP, and JMarti line model which takes the frequency characteristics into consideration is used with system model shown in Figure 6. Line parameters are as follows: line LGJ-300; the vertical distance from the line to the ground 10m. The total length of the line is 50 km with four measuring points, and the spacing between adjacent points is 10 km.

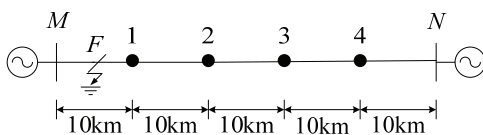


Fig. 6 Simulation model of earth fault

It is supposed that single phase earth fault occurs at 5 km from the end; the initial phase angle is 45° ; transition resistance is 10Ω ; the wavelet scale is 4; and sampling frequency is 10 MHz. It is found after data processing over the simulation signal using MATLAB that wave head of earth mode is not detected at measuring point 4, while the other three measuring points are all effective nodes and their mode transmission time delays measured are $t_1 = 0.4 \mu\text{s}$, $t_2 = 2.4 \mu\text{s}$, $t_3 = 4.6 \mu\text{s}$, respectively. As t_1 is the smallest, it can be initially judged that the fault point is near the measuring point 1, so the measuring points 2 and 3 are all located in the downstream of the fault point. Then $d_2 = 4.832 \text{ km}$, $d_3 = 5.098 \text{ km}$ can be estimated from t_2 and t_3 according to the $d-\Delta t$ curve in Figure 3. Finally, $d_F = 4.965 \text{ km}$, the fault distance from the fault point to the end M, and -35m absolute error can be derived from Formula (14).

Fault location results simulated under different fault condition are shown in Table1. It can be seen that location results are almost free from the influence of transition resistance and the initial phase angle of the fault. Even with

small angle and large transition resistance, the measurement error is still less than 500 m.

Table 2 shows the different fault location results. The results reveal that the location of different fault points can be effectively determined with high reliability using this method, and the location accuracy can properly meet the field requirements.

Table. 1 Fault location results under different fault conditions

Initial phase angle of the fault /($^\circ$)	Transition resistance / Ω	Fault distance /km	Measurement distance/km	Absolute error/km
90	10	21	21.154	0.154
36	100	21	21.154	0.154
18	1000	21	21.452	0.452

Table. 2 Fault location results at different fault points

Fault distance/km	Initial phase angle of the fault /($^\circ$)	Transition resistance / Ω	Measurement distance/km	Absolute error/km
5	45	10	4.965	-0.035
15	45	100	14.832	-0.168
28	72	500	27.715	-0.285
42	90	100	41.971	0.029

Conclusions

A traveling wave fault location method for earth faults based on mode transmission time delays using multi-measuring points is discussed in this paper. This method requires no GPS time scale, and can make full use of the delays of the arrival time for the initial traveling waves of aerial mode and earth mode. Meanwhile, comprehensive fault location can be realized based on the relationship between fault distance and mode transmission time delays. The simulation results show that this method is almost free from the influence of transition resistance and initial phase angle of fault and other factors, with high reliability. Besides, this method is also suitable for transmission lines of different length.

Acknowledgments

This work was supported by a grant from the National High Technology Research and Development Program of China (863 Program) (No. SS2012AA050803), The Science and Technology Commission of Shanghai (No. 10dz1203000) and the National Natural Science Foundation of China (No. 50977057).

REFERENCES

- [1] SUN Bo, XU Bingyin, SUN Tongjing, et al. New fault location method based on approximate entropy of transient zero-module current in non-solidly earthed network . Automation of Electric Power Systems, 2009, 33 (20) : 83-87.
- [2] LI Youjun , WANG Junsheng , ZHENG Yuping , et al . Comparison of several algorithms of travelling wave based fault location. Automation of Electric Power Systems, 2001, 25 (14) : 36-39.
- [3] ZHENG Feng, LIANG Jun, ZHANG Li, et al. Novel method about traveling wave fault location based on treble terminal measurement data for transmission line . Automation of Electric Power Systems, 2008, 32 (8) : 69-72.
- [4] Qin Jian, Chen Xiangxun, Zheng Jianchao . Study on dispersion of travelling wave in transmission line. Proceedings of the CSEE, 1999, 19(9): 28-30, 35.

- [5] LI Youjun, XU Lina. Relationship between earth mode surge and frequency on power system earth fault. *Relay*, 2007, 35(15): 4-8.
- [6] ZHANG Fan, PAN Zhencun, ZHANG Huifen, et al. New algorithm based on traveling wave for location of single phase to ground. *Proceedings of the CSEE*, 2007, 27(28): 46-52
- ZOU Jiyan, DUAN Xiongying, ZHANG Tie. The simulating calculation and experimental research of Rogowski coil for current measurement. *Transactions of China Electrotechnical Society*, 2001, 16 (1) : 81-84.
- [7] SONG Guobing, LI Sen, KANG Xiaoning, et al. A novel phase-mode transformation matrix. *Automation of Electric Power Systems*, 2007, 31 (14) : 57-60.
- [8] DONG Xinzhong, GE Yaozhong, XU Bingyin. Research of fault location based on current travelling waves. *Proceedings of the CSEE*, 1999, 19(4): 76-80.
- [9] LIN Xiangning, LIU Pei, LIU Shiming. Studies on fault location of fault-induced transient component[J]. *Automation of Electric Power Systems*, 2002, 26 (3) : 45-51.
- [10] ZHENG Zhou, LÜ Yanping, WANG Jie, et al. A new two-terminal traveling wave fault location method based on wavelet transform. *Power System Technology*, 2010, 34 (1) : 203-207.
- [11] Ge Yaozhong . *New Relay Protection and Fault Location Principle and Technology (Second Edition)*[]. Xi'an: Xi'an JiaoTong University Press, 2007.
- [12] YU Chang, YIN Xianggen, ZENG Xiangjun, et al. Fault location based on comprehensive wavelet analysis at different scales. *Electric Power Automation Equipment*, 2001, 21 (6) : 6-9.

Authors: Yadong Liu No.800, Dongchuan Rd., Minhang District, Shanghai, China, E-mail:yd@situ.edu.cn; Dr. Gehao Sheng, shenghe@situ.edu.cn; Prof. Xiuchen Jiang., xcjiang@situ.edu.cn.